

# Ultra-Compact Band-Pass Filter at Low Frequency of Operation

Basil J. Paul<sup>1, 2, \*</sup> and Shanta Mridula<sup>1</sup>

**Abstract**—An ultra-compact band-pass filter is presented in this paper. The filter is designed to operate in the medical implants communication service (MICS) band ranging from 401 MHz to 406 MHz. The filter is designed on a Rogers RT/duroid substrate with  $\epsilon_r = 2.94$  and  $\tan \delta = 0.0012$ . The overall size of the proposed filter is only  $30.6 \text{ mm} \times 18.5 \text{ mm}$  ( $0.058\lambda_g \times 0.035\lambda_g$ ), making it suitable for compact, portable devices. An equivalent circuit model is also proposed for the analysis of the filter geometry. From the circuit model, it can be concluded that the filter exhibits the characteristics of a dual-composite right left-handed (D-CRLH) transmission line. This is also confirmed from the dispersion characteristics. The salient features of the proposed filter include ultra-compactness at low operating frequency, harmonic suppression of 3.7 times of the passband frequency, fractional bandwidth of 4.45%, and good roll-off rate of 297.6 dB/GHz in the lower stopband and 116.4 dB/GHz in the upper stopband.

## 1. INTRODUCTION

Filters are widely used in communication systems to eliminate unwanted signals entering into systems. A good filter is expected to exhibit a sharp roll-off to eliminate all spurious signals and harmonic suppression with good stopband attenuation. Moreover, when the operating frequency is low, the size of the filter is also very critical in order to build compact handheld devices.

Many interesting works have already been reported in literature, presenting compact filters with harmonic suppression. In [1], a compact low pass filter with wide harmonic suppression is presented using inter-digital capacitors. Moving on to band-pass filters, again there are a variety of designs available in literature, presenting compact band-pass filters operating on a higher frequency band. In [2], a multilayer band-pass filter operating in GHz band is presented with good harmonic suppression. This has a relatively complicated multilayer geometry with a large size. In [3], a band-pass filter focusing on second harmonics suppression with triangular corrugations is presented. In [4], slot stubs are introduced to achieve harmonic suppression compromising on filter dimension. In [5], harmonic suppression is achieved in band-pass filters using spur line. In [6], split ring resonators and defected ground structures are used to achieve wide stopband. In [7, 8], fractal based geometries are used for developing band-pass filters.

However, only limited works have been reported on filters with narrow passband, especially in low frequency range. The major difficulty that can arise is to arrive at a compact geometry. Compactness in filters can be achieved using various techniques. In [9], a capacitor loaded band-pass filter with narrow passband in lower frequency range is presented with a design constraint of using discrete capacitors. In [10], a complete planar geometry is proposed for a band-pass filter operating in the lower end of ultra-high frequency (UHF) band. This has a relatively complicated geometry with larger size and slightly higher insertion loss than the proposed filter in this paper. In [11], a parallel coupled microstrip

---

*Received 28 March 2023, Accepted 10 June 2023, Scheduled 18 June 2023*

\* Corresponding author: Basil J. Paul (basiljpaul@mace.ac.in).

<sup>1</sup> Division of Electronics Engineering, School of Engineering, Cochin University of Science and Technology, Cochin, Kerala, India. <sup>2</sup> Department of Electronics and Communication, Mar Athanasius College of Engineering, Kothamangalam, Ernakulam, Kerala, India.

hairpin based band-pass filter is presented with a large filter dimension. In [12], spiral capacitors with vias are used to design a band-pass filter in MHz frequency band.

Applying the principles of metamaterials is one way to build compact microwave structures. Composite right left handed (CRLH) and dual-composite right left handed (D-CRLH) transmission lines are the commonly used approaches for transmission line implementation. In [13, 14], band-pass filters based on CRLH transmission line are presented. Compared with a CRLH transmission line, an ideal D-CRLH transmission line has the advantage of an infinitely long left handed band [15], and the proposed work focuses on developing a compact band-pass filter using a D-CRLH transmission line. In [16, 17], the concept of D-CRLH transmission line based band-pass filters with relatively wider passbands are proposed. In [18], a D-CRLH transmission line based band-pass filter with multiple notch bands is presented. This can also be used to develop band-pass filters with narrow passband. In [19, 20], a D-CRLH unit cell and its application as a narrow band-pass filter are presented, but at a relatively higher passband frequency than the proposed filter in this paper. In [21], a high frequency D-CRLH transmission line using millimeter wave integrated circuit technology is presented. In [22], a D-CRLH transmission line is realized using inductively connected split ring resonators. In [23, 24], D-CRLH based resonators are proposed. In [25], a combined filtering and antenna geometry based on D-CRLH transmission line is proposed.

In this work, the concept of D-CRLH transmission line is used to realize an ultra-compact band-pass filter with a low operating frequency band. The proposed filter is designed to operate in the Medical Implants Communication Service (MICS) band ranging from 401 MHz to 406 MHz which allows to have a close monitoring of patient parameters remotely. MICS band is highly narrow at low operating frequency, thereby making filter design more complex. The proposed filter employs a meander line inductor and interdigital capacitors to achieve compactness at the low frequency of operation. The size of the filter is only  $30.6 \text{ mm} \times 18.5 \text{ mm}$  ( $0.058\lambda_g \times 0.035\lambda_g$ ). The key merits of the filter include simple geometry, completely planar design, ultra-compact size, narrow passband with a fractional bandwidth of 4.45%, good roll-off rate of 297.6 dB/GHz in the lower stopband and 116.4 dB/GHz in the upper stopband, and a harmonic suppression up to 3.7 times of the passband frequency. The equivalent lumped circuit model of the filter is also proposed. The dispersion diagram of the filter is obtained from  $S$ -parameters. The D-CRLH transmission line characteristics of the filter are hence confirmed.

## 2. DESIGN EVOLUTION OF THE FILTER

The filter is designed on a Rogers RT/duroid substrate with  $\epsilon_r = 2.94$  and  $\tan \delta = 0.0012$ . The geometry consists of an asymmetric co-planar feed with perturbed ground on one side. Interdigital capacitors are embedded in the transmission line, and a meandered line inductor is connected between feed line and the co-planar ground plane as shown in Fig. 1. A conductor backing is provided in the bottom plane.

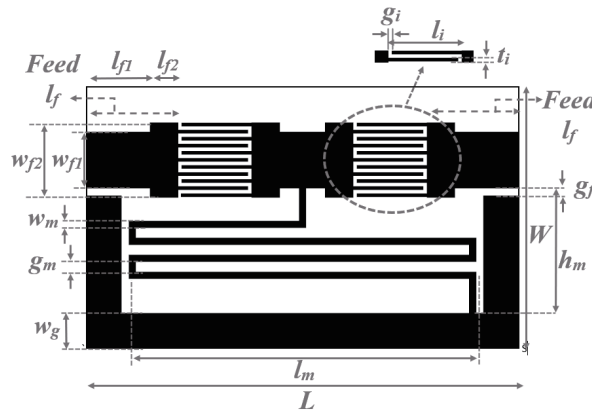


**Figure 1.** Geometry of the proposed band-pass filter.  $L = 30.6 \text{ mm}$ ,  $W = 18.5 \text{ mm}$ ,  $l_m = 24.6 \text{ mm}$ ,  $w_{f1} = 4 \text{ mm}$ ,  $w_{f2} = 5.32 \text{ mm}$ ,  $l_{f1} = 4.5 \text{ mm}$ ,  $l_{f2} = 2 \text{ mm}$ ,  $w_m = 0.5 \text{ mm}$ ,  $g_m = 0.7 \text{ mm}$ ,  $h_m = 8.825 \text{ mm}$ ,  $w_g = 2.5 \text{ mm}$ ,  $g_i = 0.25 \text{ mm}$ ,  $l_i = 4.95 \text{ mm}$ ,  $t_i = 0.25 \text{ mm}$ ,  $g_f = 0.52 \text{ mm}$ .

The dimensions are optimized for the required band of operation. The overall size of the proposed filter is only  $30.6 \text{ mm} \times 18.5 \text{ mm}$  ( $0.058\lambda_g \times 0.035\lambda_g$ ), making it suitable for compact, portable devices.

The evolution of the proposed filter geometry is shown in Fig. 2. The filter is derived from a coplanar waveguide (CPW) transmission line with an asymmetric ground on one side and conductor backing on the bottom as shown in Fig. 2(a). The ground plane is then perturbed to incorporate the meander line inductor, thereby resulting in a compact structure. This is shown in Figs. 2(b) and 2(c). Interdigital capacitors are then embedded in the transmission line as shown in Fig. 2(d). The meander line inductor and interdigital capacitors are optimized to get a transmission peak in the required MICS band. The transmission characteristics of the structure during evolution process are shown in Fig. 3.

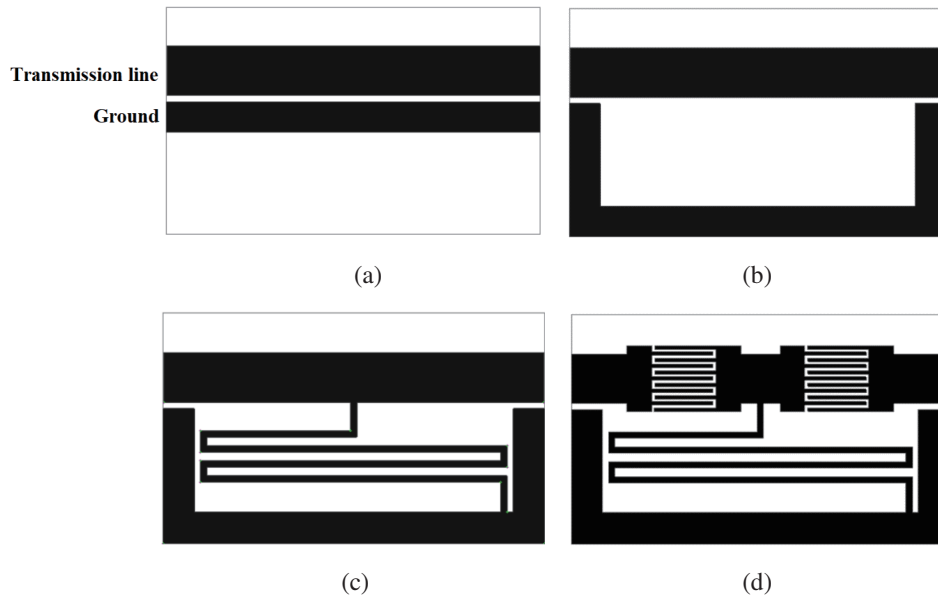


**Figure 2.** Evolution of the proposed filter. (a) CPW transmission line with an asymmetric ground on one side. (b) CPW transmission line with an asymmetric perturbed ground on one side. (c) Meander line connected between transmission line and ground. (d) Interdigital fingers embedded in the transmission line.

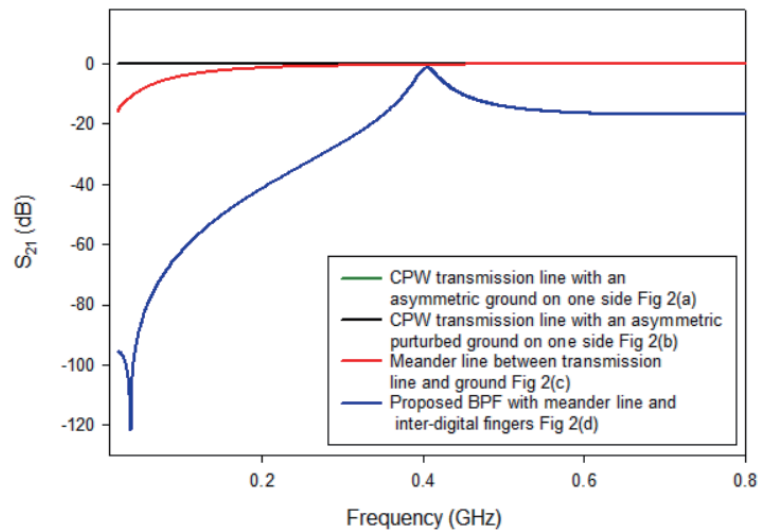


**Figure 3.** Transmission characteristics during the evolution of the proposed filter.

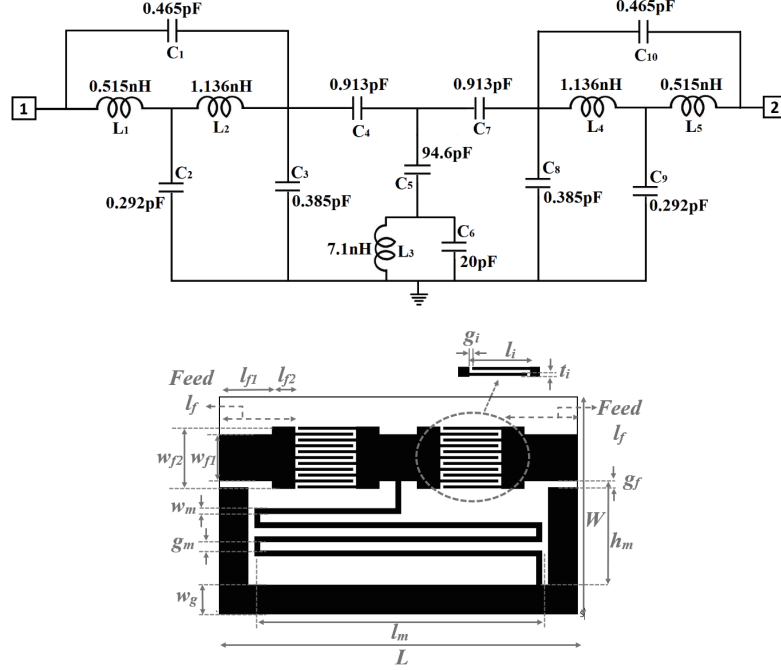


**Figure 4.** Lumped circuit model of the proposed filter. The filter geometry is also shown for reference.

### 3. LUMPED CIRCUIT MODEL OF THE FILTER

The lumped circuit model of the proposed filter is shown in Fig. 4.  $L_1$ ,  $L_2$ ,  $L_4$ ,  $L_5$  and  $C_2$ ,  $C_3$ ,  $C_8$ ,  $C_9$  represent the inductance and capacitance of the transmission line section  $l_{f1}$  and  $l_{f2}$  [26, 27].  $C_1$  and  $C_{10}$  represent the parallel plate capacitance formed by the feed  $l_f$  and the bottom conductor.  $C_4$  and  $C_7$  represent the capacitance of the interdigital fingers embedded in the transmission line, which is calculated using (1) where  $l_i$  is the length of the finger in  $\mu\text{m}$ ,  $n$  the number of fingers, and  $\epsilon_r$  the relative permittivity of the substrate [28].

$$C_4(pF) = C_7(pF) = 3.937 \times 10^{-5} l_i (\epsilon_r + 1) [0.11(n - 3) + 0.252] \quad (1)$$

$L_3$  represents the inductance of the meander line section, computed using (2), where  $h_m$  is the effective width of the meander line,  $w_m$  the width of the meander line, and  $t_m$  the thickness of the copper [29]. The dimensions are measured in cm.

$$L_3(nH) = 2l \left[ \ln \left( \frac{h_m}{w_m + t_m} \right) + 0.22 \left( \frac{w_m + t_m}{h_m} \right) + 1.19 \right] \quad (2)$$

$C_5$  and  $C_6$  represent the capacitance contributed by the meander line structure, which is modeled using (3) and (4), where  $a = w_m/2$  which is half the width of the meander line [30, 31], and the dimensions are measured in mm.

$$C_5(pF) = \left\{ \frac{12.0674 h_m}{\log \left( \frac{2h_m}{a} \right) - 0.7245} \right\} \quad (3)$$

$$C_6(pF) = 2(h_m) \left[ \frac{0.89075}{\left[ \log \left( \frac{2h_m}{a} \right) \right]^{0.8006} - 0.861} - 0.02541 \right] \quad (4)$$

### 4. DISPERSION CHARACTERISTICS OF THE FILTER

The circuit models of CRLH and D-CRLH transmission lines are shown in Fig. 5. The dispersion characteristics of these transmission lines are shown in Fig. 6. It is evident from the dispersion

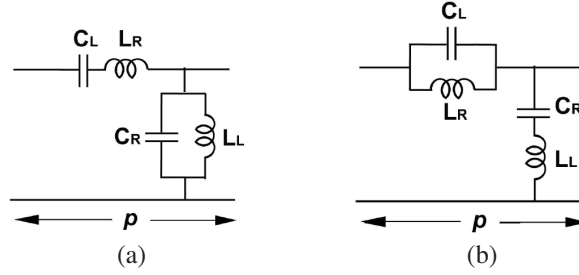


**Figure 5.** Lumped circuit model. (a) CRLH transmission line. (b) D-CRLH transmission line.

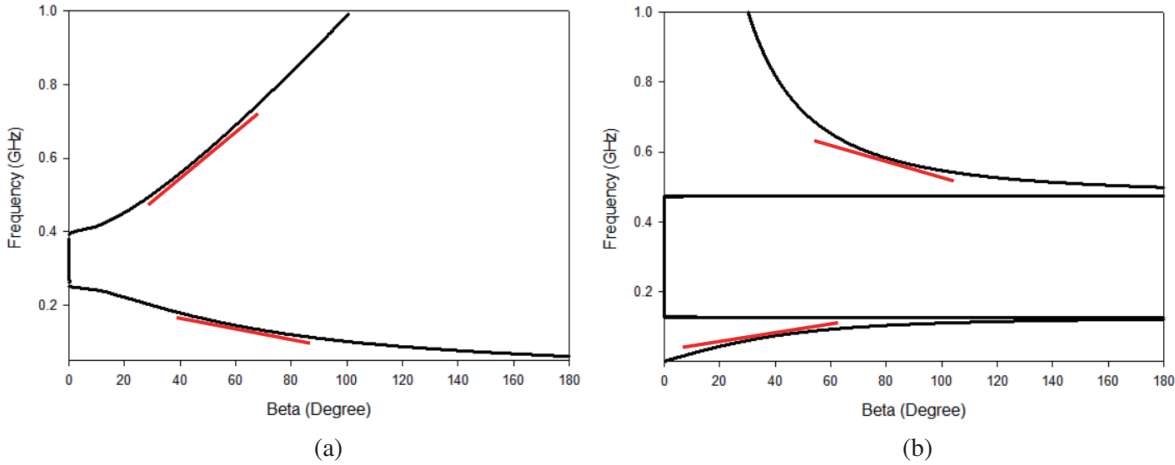


**Figure 6.** Dispersion characteristics of the lumped circuit model. (a) CRLH transmission line. (b) D-CRLH transmission line.

characteristics that a CRLH transmission line has a left handed region followed by the right handed region. This is evident from the slope of the curve marked in red line. Initially the curve has a negative slope, and later slope is positive. In the case of a D-CRLH transmission line, a positive sloped right handed region is followed by an infinitely large negatively sloped left handed region [15, 32–34].

The propagation constant  $\gamma$  and  $S$ -parameters are related using (5) and can be used for getting the dispersion characteristics [35] of the proposed filter.

$$e^{\gamma p} = \left( \frac{1 - S_{11}^2 + S_{21}^2}{2S_{21}} + K \right) \tag{5}$$

where  $K = \frac{\sqrt{(1+S_{11}^2-S_{21}^2)^2 - (2S_{11})^2}}{2S_{21}}$ .

### 5. FABRICATION, RESULTS AND DISCUSSION

The proposed filter is fabricated using conventional photolithography techniques. Photographs of the fabricated filter are shown in Fig. 7.

The return loss and transmission characteristics of the proposed filter from simulation, measurement, and lumped circuit model are shown in Fig. 8. The results are in good agreement with each other. The simulated insertion loss is  $-1.27$  dB in the passband centered at 404 MHz, and the stopband attenuation is better than  $-16$  dB. The measured insertion loss is  $-1.46$  dB in the passband, and the stopband attenuation is better than  $-16$  dB. The filter exhibits a good harmonic suppression of 3.7 times of the passband frequency.

The lumped circuit model in Fig. 4 is similar to that of the circuit model of an ideal D-CRLH transmission line shown in Fig. 5. From this similarity, it is expected that the proposed filter behaves like

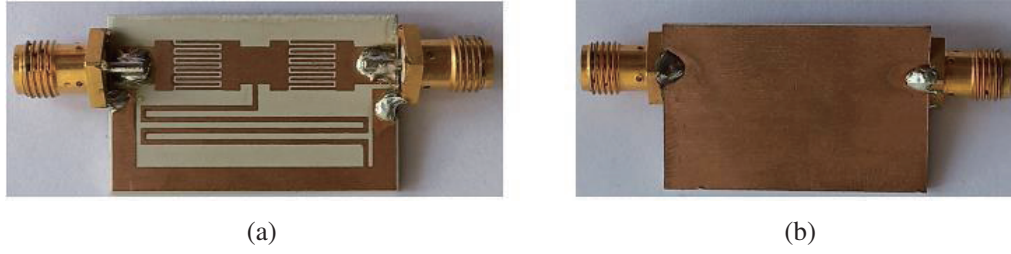


**Figure 7.** Photograph of the fabricated filter. (a) Top plane. (b) Bottom plane.

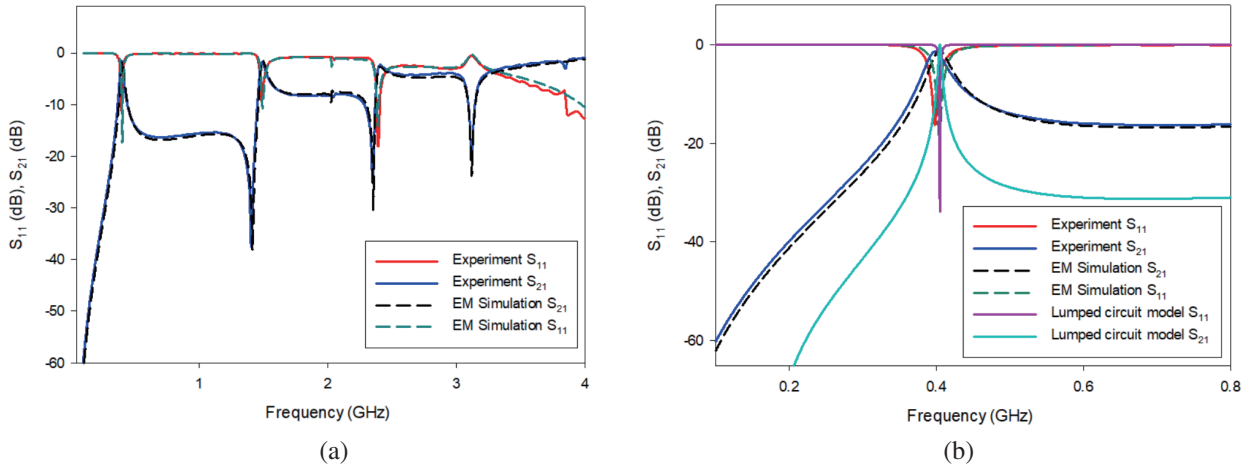


**Figure 8.** Return loss and transmission characteristics of the proposed filter from simulation, experiment and lumped circuit model. (a) Wider frequency sweep. (b) Shorter frequency sweep.

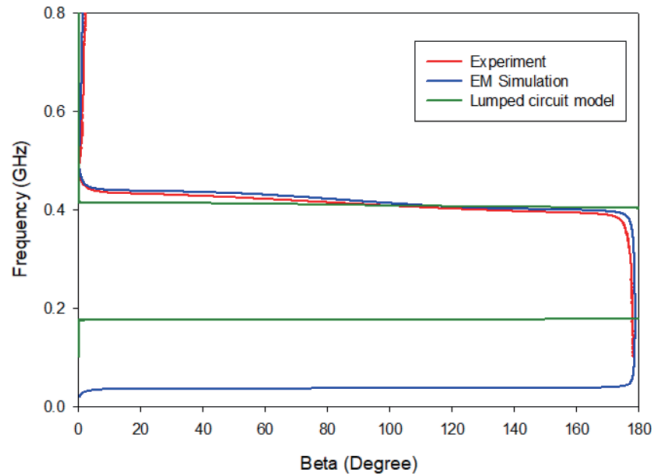


**Figure 9.** Dispersion characteristics of the proposed filter from simulation, experiment and lumped circuit model.

a D-CRLH transmission line. This can be confirmed from the dispersion characteristics of the proposed filter obtained using (5). The dispersion characteristics of the filter from simulation, experiment, and lumped circuit model are shown in Fig. 9, which again are in good agreement with each other. It is concluded that the dispersion characteristics exhibits a right handed region followed by a left handed region similar to that of a D-CRLH transmission line. The slight deviation in the characteristics of

lumped circuit model can be due to the modelling with ideal inductors and capacitors. Additionally, parasitic capacitance and inductance that can arise in electromagnetic simulation and experiment are not accounted in lumped circuit model. Instead, each element in the filter geometry is considered separately.

## 6. CONCLUSION

An ultra-compact band-pass filter with narrow passband is proposed. The filter is highly compact making it suitable for low frequency medical service band. An equivalent circuit model for the filter is proposed and analysed. It is found that the filter exhibits the property of a D-CRLH transmission line and is verified using a dispersion diagram. The salient features of the filter include simple geometry, completely planar design, ultra-compact size, narrow passband with a fractional bandwidth of 4.45% in the MICS band, good roll-off rate of 297.6 dB/GHz in the lower stopband and 116.4 dB/GHz in the upper stopband, and a harmonic suppression up to 3.7 times of the passband frequency.

## ACKNOWLEDGMENT

The authors would like to thank Kerala State Council for Science Technology and Environment (KSCSTE) for providing financial assistance for this research work as per Council File No. 03/FSHP/2013/CSTE, dated 10/01/2014.

## REFERENCES

1. Mandal, A. and T. Moyra, "Compact low-pass filter (LPF) with wide harmonic suppression using interdigital capacitor," *Frequenz*, Vol. 77, No. 1–2, 1–8, 2022.
2. Fathi, E., F. Setoudeh, and M. B. Tavakoli, "Design and fabrication of a novel multilayer bandpass filter with high-order harmonics suppression using parallel coupled microstrip filter," *ETRI Journal*, Vol. 44, No. 2, 260–273, 2021.
3. Das, T. K. and S. Chatterjee, "Improved second harmonic suppression in a compact coupled-line bandpass filter with triangular corrugations," *Microsystem Technologies*, Vol. 25, 1945–1956, 2018.
4. Idris, I. H., M. R. Hamid, K. Kamardin, M. K. A. Rahim, F. Zubir, and H. A. Majid, "Band-pass filter with harmonics suppression capability," *International Journal of Electrical and Computer Engineering*, Vol. 8, No. 4, 2512–2520, 2018.
5. Das, T. K. and S. Chatterjee, "Harmonic suppression by using T-shaped spur-line in a compact hairpin-line bandpass filter," *Radioengineering*, Vol. 30, No. 2, 296–303, 2021.
6. Chaimool, S. and P. Akkaraekthalin, "Miniaturized wideband bandpass filter with wide stopband using metamaterial-based resonator and defected ground structure," *Radioengineering*, Vol. 21, No. 2, 611–616, 2012.
7. Lotfi-Neyestanak, A. A. and A. Lalbakhsh, "Improved microstrip hairpin-line bandpass filters for spurious response suppression," *Electronics Letters*, Vol. 48, No. 14, 858–859, 2012.
8. Chen, W.-L. and G.-M. Wang, "Effective design of novel compact fractal-shaped microstrip coupled-line bandpass filters for suppression of the second harmonic," *IEEE Microwave and Wireless Components Letters*, Vol. 19, No. 2, 74–76, 2009.
9. Duraiswamy, P, "Compact capacitor-loaded tunable microstrip bandpass filter for low-frequency applications," *Journal of The Institution of Engineers (India): Series B*, Vol. 103, 1453–1457, 2022.
10. Jovanovic, S. and A. Nestic, "A new microstrip band-pass filter for UHF range," *TELSIKS 2005 — 2005 UTH International Conference on Telecommunication in Modern Satellite, Cable and Broadcasting Services*, Vol. 12005, 167–169, Nis, Serbia, 2005.
11. Hasan, A. B., M. T. Rahman, A. Kahhar, T. Trina, and P. K. Saha, "Design of miniature type parallel coupled microstrip hairpin filter in UHF range," *AIP Conference Proceedings*, Vol. 1919, 020017-1–020017-7, 2017.

12. Peng, L. and X. Jiang, "Ultra-compact UHF band-pass filter designed by archimedes spiral capacitor and shorted-loaded stubs," *Frequenz*, Vol. 69, Nos. 1–2, 71–73, 2014.
13. Jang, G. and S. Kahng, "Compact metamaterial zeroth-order resonator bandpass filter for a UHF band and its stopband improvement by transmission zeros," *IET Microw. Antennas Propag.*, Vol. 5, No. 10, 1175–1181, 2011.
14. Choudhary, D. K. and R. K. Chaudhary, "A compact via-less metamaterial wideband bandpass filter using split circular rings and rectangular stub," *Progress In Electromagnetics Research Letters*, Vol. 72, 99–106, 2018.
15. Caloz, C., "Dual composite right left handed (D-CRLH) transmission line metamaterial," *IEEE Microwave and Wireless Components Letters*, Vol. 16, No. 11, 585–587, 2006.
16. Garg, P. and P. Jain, "Design and analysis of a bandpass filter using dual composite right/left handed (D-CRLH) transmission line showing bandwidth enhancement," *Wireless Personal Communications*, Vol. 120, 1705–1720, 2021.
17. Hoseini, S. M. S. N., R. Zaker, and K. Monfaredi, "A microstrip folded compact wideband bandpass filter with wide upper stopband," *ETRI Journal*, Vol. 43, No. 6, 957–965, 2021.
18. Wu, G.-C., G.-M. Wang, and Y.-W. Wang, "Novel simplified dual-composite right/left handed transmission line and its application in bandpass filter with dual notch bands," *Progress In Electromagnetics Research C*, Vol. 44, 123–131, 2013.
19. Shen, G., X. Wang, W. Che, W. Feng, W. Yang, and K. Deng, "Miniaturized high-performance D-CRLH resonator and filter based on accurate equivalent circuit model," *International Workshop on Electromagnetics: Applications and Student Innovation Competition (iWEM)*, 1–3, Hsinchu, Taiwan, 2015.
20. Shen, G., W. Che, Q. Xue, and W. Yang, "Characteristics of dual composite right/left-handed unit cell and its applications to bandpass filter design," *IEEE Transactions on Circuits and Systems II: Express Briefs*, Vol. 65, No. 6, 719–723, 2018.
21. Tong, W., Z. Hu, H. Zhang, C. Caloz, and A. Rennings, "Study and realisation of dual-composite right/left-handed coplanar waveguide metamaterial in MMIC technology," *IET Microwaves, Antennas & Propagation*, Vol. 2, No. 7, 731–736, 2008.
22. Belenguer, A., J. Cascon, A. L. Borja, H. Esteban, and V. E. Boria, "Dual composite right-/left-handed coplanar waveguide transmission line using inductively connected split-ring resonators," *IEEE Transactions on Microwave Theory and Techniques*, Vol. 60, No. 10, 3035–3042, 2012.
23. Daw, A. F., P. A. Fawzey, and M. N. Adly, "Quad-band resonator depends on CRLH/D-CRLH structures," *Microwaves & RF (MWRF)*, October 2019, available online: <https://www.mwrf.com/technologies/components/article/21849975/quadband-resonator-depends-on-crlhdcrlh-structures>.
24. Daw, A. F., M. A. Abdalla, and H. M. Elhennawy, "New configuration for multiband ultra compact gap resonator based D-CRLH," *IEEE Middle East Conference on Antennas and Propagation (MECAP)*, 1–4, 2016.
25. Abdalla, M. A. and A. Fouad, "Integrated filtering antenna based on D-CRLH transmission lines for ultra-compact wireless applications," *Progress In Electromagnetics Research C*, Vol. 66, 29–38, 2016.
26. Paul, B. J., S. Mridula, B. Paul, and P. Mohanan, "Metamaterial inspired CPW fed compact low-pass filter," *Progress In Electromagnetics Research C*, Vol. 57, 173–180, 2015.
27. Paul, B. J., S. Mridula, A. Pradeep, and P. Mohanan, "Design of an ultra compact antenna for low frequency applications," *Progress In Electromagnetics Research Letters*, Vol. 105, 95–102, 2022.
28. Hong, J.-S., *Microstrip Filters for RF/Microwave Applications*, John Wiley & Sons, 2011.
29. Varadan, V. K., K. J. Vinoy, and K. A. Jose, *RF MEMS and Their Applications*, John Wiley & Sons, 2003.
30. Olaode, O. O., W. D. Palmer, and W. T. Joines, "Effects of meandering on dipole antenna resonant frequency," *IEEE Antennas and Wireless Propagation Letters*, Vol. 11, 122–125, 2012.

31. Olaode, O. O., W. D. Palmer, and W. T. Joines, "Characterization of meander dipole antennas with a geometry-based, frequency-independent lumped element model," *IEEE Antennas and Wireless Propagation Letters*, Vol. 11, 346–349, 2012.
32. Caloz, C. and T. Itoh, *Electromagnetic Metamaterials: Transmission Line Theory and Microwave Applications*, John Wiley & Sons, 2006.
33. Ryu, Y.-H., J.-H. Park, J.-H. Lee, J.-Y. Kim, and H.-S. Tae, "DGS dual composite right/left handed transmission line," *IEEE Microwave and Wireless Components Letters*, Vol. 18, No. 7, 434–436, 2008.
34. Lu, K., G.-M. Wang, and B. Tian, "Design of dual-band branch-line coupler based on shunt open-circuit DCRLH cells," *Radioengineering*, Vol. 22, No. 2, 618–623, 2013.
35. Eisenstadt, W. R. and Y. Eo, "S-parameter-based IC interconnect transmission line characterization," *IEEE Transactions on Components, Hybrids, and Manufacturing Technology*, Vol. 15, No. 4, 483–490, 1992.